A Negative Conductivity Material Makes a dc Invisibility Cloak Hide an Object at a Distance

Fan Yang, Zhong Lei Mei, Xin Yu Yang, Tian Yu Jin, and Tie Jun Cui**

The theoretical design and the first experimental verification of an exterior dc invisibility cloak that can hide an object from dc detection at a distance are presented. Based on the transformation optics theory, the exterior dc cloak requires negative conductivity material to create folded geometry, which will cancel the real geometry of detected object in distance and make it invisible. Negative conductivities are designed and realized using active devices, together with resistor networks, to generate the equivalent conductivity materials required by the exterior dc cloak. An experimental sample of the dc cloak is fabricated on the printed circuit board and the measured result has excellent agreement with numerical and circuit simulations, showing very good cloaking performance at a distance.

1. Introduction

Recently, invisibility cloaks have attracted great attentions due to their significant impacts on science and engineering, and increasing progress has been achieved in both theory and experiment. Since Pendry proposed the transformation optics (TO) theory in 2006,[1] many kinds of invisibility cloaks have been realized in different frequency bands.[2–13] Generally speaking, the invisibility cloaks are classified into three types: closed cloaks, carpet cloaks, and exterior cloaks. The closed cloak is covered around the detected target in free space and makes the target inside invisible.[1] The carpet cloak is designed to hide an object on the ground plane.[3] When the carpet cloak is covered above the ground plane, it makes the object underneath invisible. In the past few years, the experimental verifications to both closed and carpet cloaks have been investigated.[2,4–12]

The exterior invisibility cloak was first theoretically presented by Lai et al. based on TO,[13] which is placed apart from the detected object and hides the object at a distance, and hence may have advantages in some specific situations. Exterior cloaks based on active sources have also been suggested.[14,15] In this scheme, a region can be cloaked from a known incident wave (an obvious weak point) by surrounding it with active devices that cancel out the field in the cloaked region without radiating waves significantly.[14,15] An indirect experimental verification to the exterior cloak was given by Li et al. using the inductor-capacitor circuits,[16] in which an illusion-optics device was designed by the complementary and restoring media to transform one object into another. However, the direct experiment on the exterior cloak is still unavailable.

Besides the invisibility cloaks for the time-varying electromagnetic fields in the microwave, optical, and terahertz frequencies,[1–16] the static invisibility cloaks in the zero frequency have also been investigated using the conducting materials or superconductors.[17–23] Based on the theoretical design,[18] two experiments on dc magnetic cloaks have recently been conducted by two groups independently using superconducting material.[22,23] In the meantime, another approach was proposed to realize a dc electric invisibility cloak with the aid of resistor network.[24] All above researches are focused on the closed dc cloaks,[17–24] but the proposed method in ref. [24] has been extended to achieve dc carpet cloak,[25] dc illusion device,[26] dc concentrator,[27] and ultrathin closed dc cloak.[28] However, the exterior dc cloak is not reported by either theory or experiment. A big challenge is due to the nonexistence of the negative conductivity in nature.

In this work, we propose the theoretical design and experimental verification to the exterior dc cloak. Based on the TO theory, negative conductivity materials are required in the device. We present a circuit model with active devices to mimic the negative electric conductivity. Using such a model and analogy between conducting materials and resistor network, we fabricate a dc exterior invisibility cloak. Nearly perfect cloaking effect is observed in experiments.

2. The Principle of a dc Exterior Cloak

The principle of the dc exterior cloak is demonstrated in **Figure 1**, in which Figure 1a shows the parallel current lines flowing in an isotropic and homogeneous background conducting material. When an object with different conductivity from the background (the yellow sphere) exists, the original current lines will be interfered significantly, as illustrated in Figure 1b. In order to hide the object, i.e., to restore the original

F. Yang, Prof. Z. L. Mei, X. Y. Yang, T. Y. Jin
School of Information Science and Engineering
Lanzhou University
Lanzhou 730000, China
E-mail: meizl@lzu.edu.cn
Prof. T. J. Cui
State Key Laboratory of Millimeter Waves
Department of Radio Engineering
Southeast University
Nanjing 210096 China
E-mail: tjcui@seu.edu.cn

DOI: 10.1002/adfm.201300226

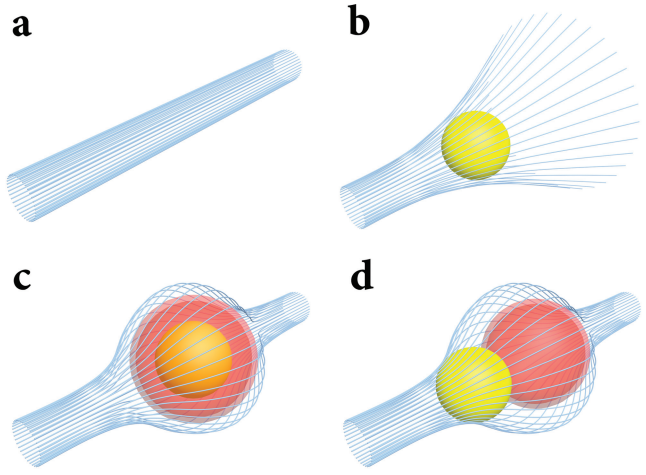

Figure 1. The principle of dc invisibility cloaks. a) The current flowing in an isotropic and homogeneous conducting material background. b) The current distribution when an object (the yellow sphere) is embedded in the background. c) The current distribution when the object is wrapped by a dc closed cloak (the red spherical shell). d) The current distribution when the object is close to a dc exterior cloak (the red spherical shell).

current lines and restrict the distortion in a limited region, two kinds of cloaks can be used: the closed cloak and exterior cloak. In Figure 1c, we wrap the detected object using a closed dc cloak (the red spherical shell); while in Figure 1d, we put a dc exterior cloak (the red spherical shell) near the detected object. In both cases, the incident current lines are guided around the object and return to their original directions outside the cloaked region as if nothing has happened. Inside the cloaked region, however, different strategies happen, as shown in Figure 1c,d.

Using the TO theory, the dc exterior invisibility cloak can be easily designed by folding a bigger spherical shell into a smaller one while keeping their common surface unchanged. In the two-dimensional case, as studied in this work and illustrated in **Figure 2**a, a larger annulus ($b < r < c$, cloaked region) is folded onto a smaller one ($a < r < b$, complementary region). At the same time, the larger circle with radius c is linearly changed into a smaller one with radius a. The linear transformation function, which involves the folding operation,[13] is shown as follow

$$\rho' = f(\rho) = \begin{cases} \frac{a}{c}\cdot\rho & 0<\rho<c \\ -\frac{b-a}{c-b}\cdot(\rho-b)+b & b<\rho<c \end{cases}, \varphi' = \varphi, z' = z, \quad (1)$$

in the cylindrical coordinates. Note that a and b represent the inner and outer radii of the cloak, and b and c are the inner and outer radii of the cloaked region. The transformation function is plotted in Figure 2b.

Assume that the conductivities of the background material and cloaked region are σ_0 and σ_m, which may be inhomogeneous and vary with the position. Then the transformed conductivity of the invisibility cloak is written as

$$\sigma' = \begin{cases} \Lambda\left[1,1,(\frac{c}{a})^2\right]\sigma_0 & 0<\rho<c, 0<\rho'<a \\ \Lambda\left[-\frac{b-a}{c-b}\cdot\frac{\rho}{\rho'},-\frac{c-b}{b-a}\cdot\frac{\rho'}{\rho},-\frac{c-b}{b-a}\cdot\frac{\rho}{\rho'}\right]\sigma_m & b<\rho<c, a<\rho'<b \end{cases} \quad (2)$$

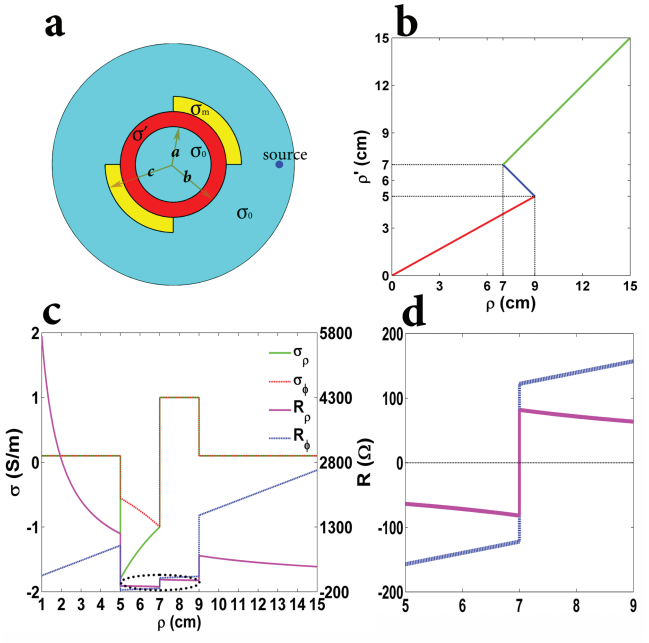

Figure 2. Schematics of the exterior cloak design and the required transformation function and parameters. a) Schematics of the exterior cloak. b) The transformation function used in the design. c) The conductivity and resistance profiles required by the dc exterior cloak. d) The zoomed region with negative resistance for the dc exterior cloak.

Hence the conductivity of the cloak is anisotropic and inhomogeneous. Though it is difficult to realize continuous anisotropic conductivities, we can use polar grid resistor networks to achieve this task.[24] The relation between the material conductivity and the resistor in the network is given by

$$R_\rho = \frac{\Delta\rho}{\sigma_\rho \rho\Delta\varphi h}, \quad R_\varphi = \frac{\rho\Delta\varphi}{\sigma_\varphi \Delta\rho h} \quad (3)$$

where R_ρ and R_φ are two components of each cell in the network. In Equation (3), $\Delta\rho$ and $\Delta\varphi$ are step lengths in the radial and tangential directions, σ_ρ and σ_φ are the radial and tangential components of the conductivity, and h represents the thickness of the continuous material in the z direction. Hence, the anisotropic conductivity can be realized using different resistors in different directions.

As the transformation suggests, the design of exterior cloaks involve the "folded geometry", which will lead to negative parameters during the transformation. In the dc case, we need negative conductivity, or equivalently, the negative resistance. In Figure 2c, we demonstrate the conductivity and resistance profiles required by the dc exterior cloak, which are anisotropic and inhomogeneous. The details of the resistance profiles for R_ρ and R_φ are given in Figure 2d when the radius is between 5 cm and 7 cm. We clearly notice that the conductivity and resistance are below zero in this region. To realize the negative conductivity and resistance, a negative resistor model is presented in **Figure 3**a, which consists of two resistors and a controlled voltage source. Here, I represents the current running through the negative resistor, μV_C stands for the electromotive force of the controlled voltage source, μ is the controlling ratio,

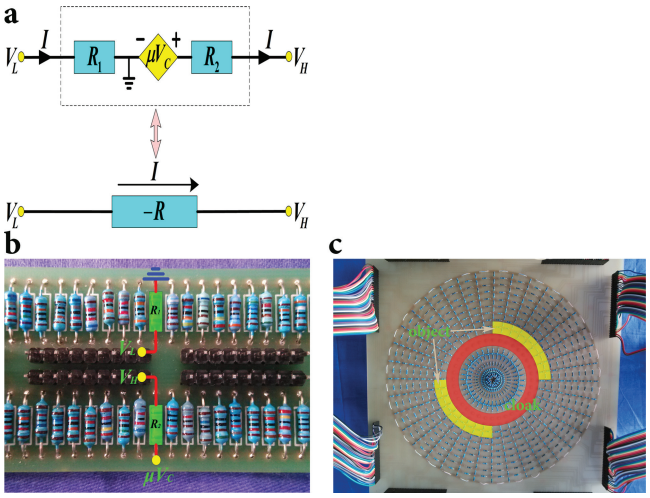

Figure 3. The negative-resistor model and fabricated sample of the exterior cloak. a) The negative-resistor model to realize negative conductivity and resistance. b) The realization of negative conductivity and resistance using resistors and active devices. c) The photograph of the fabricated dc exterior cloak, which is constructed by the resistor network in the polar grids.

and V_C is the voltage of excitation in the network. Resistors R_1 and R_2 are used to match the current and voltage of the port, while V_H and V_L denote the high and low voltages, respectively, and $-R$ is the resistance of the ideal negative resistor. Since the current I running through $-R$ is $(V_H - V_L)/R$, and the proposed model is used to replace the ideal negative resistor, we can easily obtain the resistances of R_1 and R_2 as

$$R_1 = \frac{V_L}{I}, \quad R_2 = \frac{\mu V_C - V_H}{I} \tag{4}$$

Because the network we fabricated is composed of linear components, the current and voltage at each node in the network change proportionally with the excitation signal, making R_1 and R_2 unchanged. Hence the model can be used to mimic an ideally negative resistor. In the design process, the negative conductivity is first calculated using Equation (2), and then mapped to the negative resistors using Equation (3) on a polar grid. Next, a circuit simulation is performed on the resulting resistor network with ideal negative-resistors, which gives the voltage and current distributions at each node, including V_H, V_L, and I mentioned above. Finally, Equation (4) is used to give the corresponding resistors in the circuit model. We remark that μ is a fixed value depending on the active sources available at hand in this process. Figure 3b illustrates the experimental realization of the negative resistor, in which a unit cell is highlighted by green colors. Considering the relatively large size of each cell, the negative resistors are not placed directly in the cloaking shell in the fabricated network, which is shown as the red annulus in Figure 3c. Instead, they are connected to the resistor network using wires.

3. Simulations and Experimental Results

Based on the above principle, we fabricate a sample of the dc exterior cloak, as shown in Figure 3c. The cloaked objects are chosen as two quarter-circular rings (see the yellow parts in Figure 2a and Figure 3c) since this configuration makes the objects look more exterior. In our design, the background material has a conductivity of 0.1 S/m, the conductivity of the cloaked region is deliberately set to 1 S/m for the two cloaked quarter rings and 0.1 S/m for the remaining part, which lead to an inhomogeneous σ_m in Equation (2). The conductivity tensor of the cloak is obtained from the same equation. The polar-grid network shown in Figure 3c is composed of 15 × 36 unit cells, i.e., 15 concentric layers in the radial direction and 36 nodes in the tangential direction. The cloaking region, which covers from the 5th to 7th layers, is a closed ring with the inner radius a = 5 cm and outer radius b = 7 cm; while the region of two quarter-circular rings are from the 7th to 9th layers with inner radius b = 7 cm and outer radius c = 9 cm. The central region inside the cloak has homogeneous and isotropic conductivity, which is clearly demonstrated in Equation (2). A point source with 5 V magnitude is connected to the network at the 14th layer.

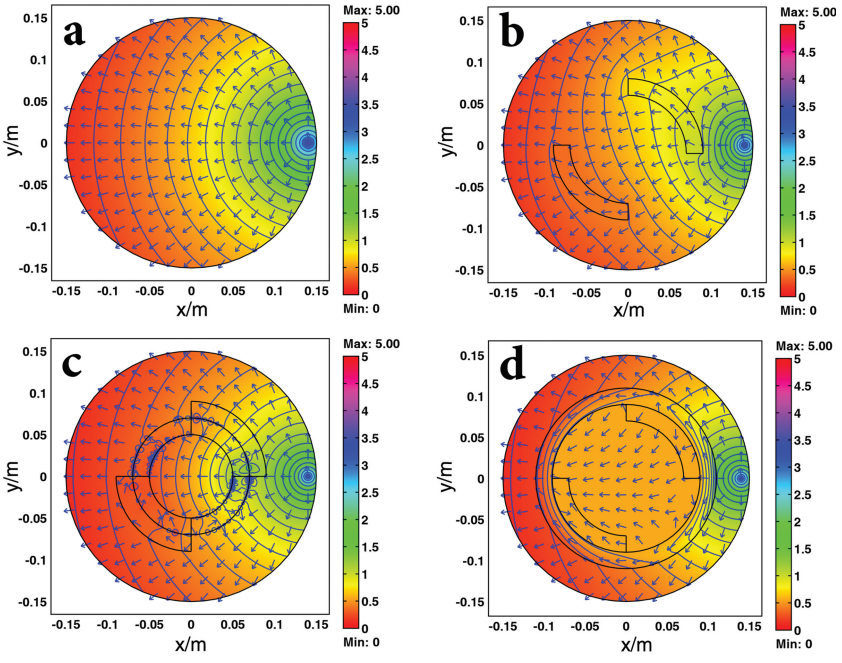

Figure 4. The numerical simulation results for the dc invisibility cloaks with continuous conductivity materials. a) The voltage and current distributions when a point source lies in the isotropic and homogeneous background material, in which the concentric circles represent the ideal equi-potential lines and the arrow represents the currents from the point source. b) The voltage and current distributions when the cloaked objects, two quarter-circular rings, are embedded in the background. c) The voltage and current distributions when the designed dc exterior cloak is placed close to the objects. d) The voltage and current distributions when the two objects are wrapped by a dc closed cloak.

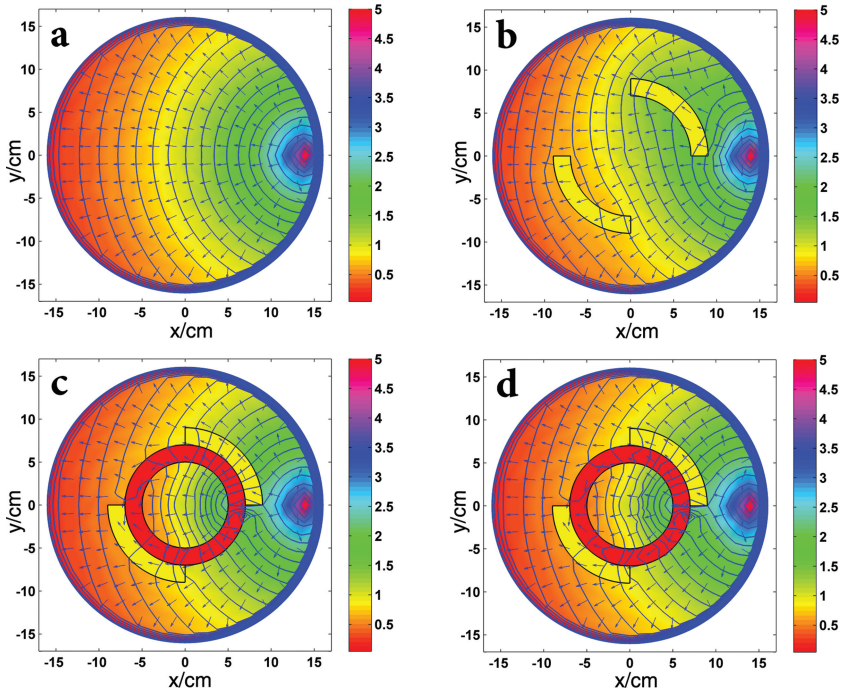

Figure 5. The circuit simulation (ADS) and measurement results of the dc exterior cloak. a) The simulated voltage and current distributions when a point source lies in the isotropic and homogeneous background, in which the concentric circles represent the ideal equi-potential lines and the arrow represents the currents from the point source. b) The simulated voltage and current distributions when the cloaked objects are embedded in the background. c) The simulated voltage and current distributions when the designed dc exterior cloak is placed close to the objects. d) The measured voltage and current distributions when the designed dc exterior cloak is placed close to the objects.

We first make full-wave simulations of the dc exterior cloak and compare its performance to the closed dc cloak.[24] The simulations are performed using the commercial software, Comsol Multiphysics, with continuous conductivity materials. **Figure 4**a illustrates the potential and current distributions when the point source exists in empty background. It is obvious that the equipotential lines are concentric circles and the arrows, which indicate the currents, are in the radial direction from the point source. When the cloaked objects are embedded into the background material, the simulation results are given in Figure 4b, from which we notice that the original potential lines are distorted and the currents become unordered due to the change of conductivity, making the objects visible to the detector. To prevent the cloaked objects from detection, we put the dc exterior cloak near the objects. In this case, the simulation results are illustrated in Figure 4c, presenting that the potential lines and the current arrows outside the cloak restore to their original distributions. For the sake of comparison, we also provide the simulation results with a dc closed cloak, as plotted in Figure 4d, which shows the same performance outside the cloaked region but with different strategies inside. To cover the objects, we note that the size of closed cloak is much larger than its exterior counterpart.

For realization, the continuous conductivity material is discretized and mimicked by a resistor network with both positive and negative resistances, as shown in Figure 3c. This circuit is numerically simulated using the commercial software, Agilent Advanced Design System (ADS), and the circuit simulation results are demonstrated in **Figure 5**. Here, we first obtain the voltage at each node in the resistor network to get the voltage distribution, from which we calculate the current distribution using the gradient of voltage. Figure 5a–c illustrates the potential and current distributions of the point source in the empty background, the background containing the objects only, and the background containing the objects and dc exterior cloak simultaneously, which have excellent agreements to those of continuous materials shown in Figure 4a–c, confirming the correctness of the equivalent resistor network. The detailed resistances (positive and negative) used in the circuit simulations are given in Section 1 and 2 in the Supporting Information.

The measured results are presented in Figure 5d. A comparison between Figure 5d and Figure 4c and 5c clearly indicates the excellent cloaking performance and experimentally verifies the functionality of the dc exterior cloak. Quantitatively speaking, the relative errors between the circuit simulation and experiment are less than 10%. The small difference is mainly attributed to the discrepancy between the available resistance we used in the experiment and the theoretical one (see Section 2 and 3 in the Supporting Information).

4. Conclusions

We have proposed the theoretical design of dc exterior cloak and made the first experimental verification. In the practical realization, we presented a key method to generate negative conductivity materials using the negative-resistor model. The cloak we fabricated can hide the object outside from being detected, and the cloaking performance is nearly perfect in both simulation and experiment results. We remark that the design can also be extended to three dimensions and other static-field active devices.

5. Experimental Section

In the circuit simulations and real experiments, some special treatments have to be conducted to handle the boundaries. In our experimental setup, the 7th layer is the interface of the cloaked objects (or the background material) and the cloak. As the transformation formula in Equation (1) suggests, the radius b is kept unchanged in the folding transformation. That is to say, the 7th layer is a superimposed layer between the cloak and cloaked objects (or background). In view of the network unit cell model we have adopted, the two resistors $R_\rho(7_+)$ and $R_\rho(7_-)$ at the 7th layer are connected in series, while those of R_φ are

connected in parallel, and the calculated resistances are $R_\rho(7) = 0$ and $R_\varphi(7) = \infty$.

Supporting Information

Supporting Information is available from the Wiley Online Library or from the author.

Acknowledgements

This work was supported in part by a Major Project of the National Science Foundation of China under Grant Nos. 60990320 and 60990324, in part by the 111 Project under Grant No. 111-2-05, and in part by National High Tech (863) Projects under Grant Nos. 2011AA010202 and 2012AA030402. Z.L.M. acknowledges the Natural Science Foundation of Gansu Province (No. 1107RJZA181), the Chunhui Project (No. Z2010081), and the Fundamental Research Funds for the Central Universities (No. LZUJBKY-2012-49, No. LZUJBKY-2013-k06).

Received: January 20, 2013
Revised: February 14, 2013
Published online: April 11, 2013

[1] J. B. Pendry, D. Shurig, D. R. Smith, *Science* **2006**, *312*, 1780.
[2] D. Schurig, J. J. Mock, B. J. Justice, S. A. Cummer, J. B. Pendry, A. F. Starr, D. R. Smith, *Science* **2006**, *314*, 977.
[3] J. Li, J. B. Pendry, *Phys. Rev. Lett.* **2008**, *101*, 203901.
[4] R. Liu, C. Ji, J. J. Mock, J. Y. Chin, T. J. Cui, D. R. Smith, *Science* **2009**, *323*, 366.
[5] J. Valentine, J. Li, T. Zentgraf, G. Bartal, X. Zhang, *Nat. Mater.* **2009**, *8*, 568.
[6] L. H. Gabrielli, J. Cardenas, C. B. Poitras, M. Lipson, *Nat. Photonics* **2009**, *3*, 461.
[7] H. F. Ma, W. X. Jiang, X. M. Yang, X. Y. Zhou, T. J. Cui, *Opt. Express* **2009**, *17*, 19947.
[8] T. Ergin, N. Stenger, P. Brenner, J. B. Pendry, M. Wegener, *Science* **2010**, *328*, 337.
[9] H. F. Ma, T. J. Cui, *Nat. Commun.* **2010**, *1*, 21.
[10] X. Chen, Y. Luo, J. Zhang, K. Jiang, J. B. Pendry, S. Zhang, *Nat. Commun.* **2011**, *2*, 176.
[11] B. Zhang, Y. Luo, X. Liu, G. Barbastathis, *Phys. Rev. Lett.* **2011**, *106*, 033901.
[12] Y. J. Bao, C. He, F. Zhou, C. Stuart, C. Sun, *Appl. Phys. Lett.* **2012**, *101*, 031910.
[13] Y. Lai, H. Y. Chen, Z. Q. Zhang, C. T. Chan, *Phys. Rev. Lett.* **2009**, *102*, 093901.
[14] F. G. Vasquez, G. W. Milton, D. Onofrei, *Opt. Express* **2009**, *17*, 14800.
[15] F. G. Vasquez, G. W. Milton, D. Onofrei, *Phys. Rev. Lett.* **2009**, *103*, 073901.
[16] C. Li, X. Liu, G. C. Liu, F. Li, G. Y. Fang, *Appl. Phys. Lett.* **2011**, *99*, 084104.
[17] A. Greenleaf, M. Lassas, G. Uhlmann, *Physiol. Meas.* **2003**, *24*, 413.
[18] B. Wood, J. B. Pendry, *J. Phys. Condens. Matter* **2007**, *19*, 076208.
[19] T. Chen, C.-N. Weng, J.-S. Chen, *Appl. Phys. Lett.* **2008**, *93*, 114103.
[20] F. Magnus, B. Wood, J. Moore, K. Morrison, G. Perkins, J. Fyson, M. C. K. Wiltshire, D. Caplin, L. F. Cohen, J. B. Pendry, *Nat. Mater.* **2008**, *7*, 295.
[21] A. Sanchez, C. Navau, J. Prat-Camps, D. Chen, *New J. Phys.* **2011**, *13*, 093034.
[22] S. Narayana, Y. Sato, *Adv. Mater.* **2012**, *24*, 71–74.
[23] F. Gömöry, M. Solovyov, J. Šouc, C. Navau, J. Prat-Camps, A. Sanchez, *Science* **2012**, *335*, 1466.
[24] F. Yang, Z. L. Mei, T. Y. Jin, T. J. Cui, *Phys. Rev. Lett.* **2012**, *109*, 053902.
[25] Z. L. Mei, Y. S. Liu, F. Yang, T. J. Cui, *Opt. Express.* **2012**, *20*, 25758.
[26] M. Liu, Z. L. Mei, X. Ma, T. J. Cui, *Appl. Phys. Lett.* **2012**, *101*, 051905.
[27] W. X. Jiang, C. Y. Luo, H. F. Ma, Z. L. Mei, T. J. Cui, *Sci. Rep.* **2012**, *2*, 956.
[28] W. X. Jiang, C. Luo, Z. L. Mei, T. J. Cui, *Appl. Phys. Lett.* **2013**, *102*, 014102.